Finite Element Updating for High Precision Space Reflector Model Using Multiobjective Optimization

Finite Element Updating for High Precision Space Reflector Model Using Multiobjective Optimization

By Takayuki OKABE[1)], Nozomu KOGISO[1)] Hiraku SAKAMOTO[2)] and Hiroaki TANAKA[3)]

[1)]*Department of Aerospace Engineering, Osaka Prefecture University, Sakai, Japan*

[2)]*Department of Mechanical and Aerospace Engineering, Tokyo Institute of Technology, Tokyo, Japan*

[3)]*Department of Aerospace Engineering, National Defence Academy of Japan, Yokosuka, Japan*

This study proposes a finite element updating method using multiobjective optimization method to consider multiple experimental conditions for estimating parameters. The method is applied to the BBM model for the tension-stabilized space reflector consisting of hoop cables and radial ribs, where the rib is deformed into the prescribed shape by cable tension generated on deployment. The design requirement is to deform the rib to the prescribed shape by appropriately applied tension loads to the radial and hoop cables. Under actual situations, the deformation shape is deviated from the ideal shape due to uncertainties. It is necessary to estimate the physical parameters in high accuracy to investigate the effect of the parameters on the deformation shape through a geometrically nonlinear finite element analysis. In order to efficiently estimate the physical parameters, the satisficing trade-off method (STOM) is adopted as a multiobjective optimization method. Numerical examples demonstrate the validity of the proposed method that the analytical deformation shapes are compared with the experimental results.

Key Words: Finite element updating, High precision space structure, multiobjective optimization, Satisficing trade-off method

1. Introduction

Space antenna for space exploration missions require large aperture areas and high surface shape accuracy, as well as lightweightness. [1)] As a large-scale highly precise space reflector structure, a tension-stabilized space reflector consisting of hoop cables and radial ribs as shown in Fig. 1 was proposed to satisfy these requirements. [2)] The ribs are arranged in the radial direction from a central hub and simply supported at the hub. The ribs are deformed to the bending deformation under tensions of hoop and tie cables on deployment, where the ribs were originally straight form in folding position. The dimensions of ribs are determined such that the bending deformation will get close to the ideal parabola shape.

The structural design is verified through the one-dimensional rib model shown in Fig. 2. [2)-4)] The one-dimensional model consists of a single rib taken from the whole reflector and a cable element that represents the tie cable. The root of the rib is simply supported, and the lower end of the tie cable is fixed in the vertical direction and free to move in the longitudinal direction. The hoop cable tension is modeled as a concentrated nodal load that deforms the rib into the ideal parabola shape from the original straight form. The deformation transfers the tension force to the tie cable as a reaction force.

Highly precise structure requires highly accurate numerical analysis to obtain the deformed shape such as a structural nonlinear finite element analysis. For the accurate analysis, the structural parameters such as stiffness and internal stress should be also estimated with high accurately. For the purpose, part of the authors proposed the accurate parameter estimation method to establish the highly accurate numerical analysis model for the tension-stabilized structure. [5)] Though the finite element updating has usually applied to the linear finite element analysis, [6), 7)] the previous study applied to the geometrically nonlinear finite element analysis. Because the analysis of tension-

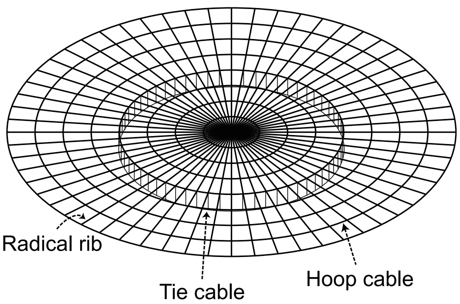

Fig. 1. Reflector consisting of radial ribs and hoop cables

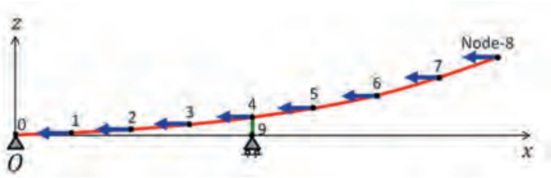

Fig. 2. Simplified one-dimensional structural model taken from the whole reflector

stabilized space structures usually requires a geometrically nonlinear analysis. In these structures, the balance of internal forces determines the structural shape, and the shape determines the distribution of internal forces; therefore, internal forces and deformation should be solved simultaneously. The structural parameters are estimated using the finite element updating that uses results of the shape measurement experiment. The experimental setup is shown in Fig, 3. The present experimental setup has only one layer of the hoop cables as the simplest representation of the tension-stabilized structure concept.

By updating the parameters with high sensitivity with respect to the rib deformation, the deformation error between the experimental and FEM results was reduced. However, the cable tension estimated by the finite element updating is much different from that of the experimental results. It is found that

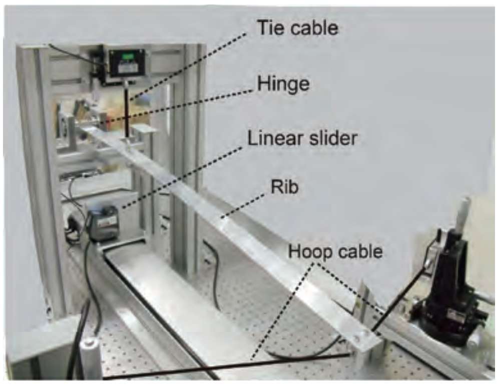

(a) Experimental system

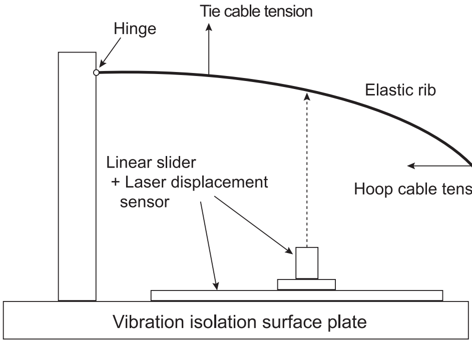

(b) Schematic figure of experimental system

Fig. 3. The overview of Experimental system

the additional experiments that gives known perturbation to the structure are efficient to reduce the errors. [5]

The previous research concludes that the efficient updating method corresponding to the multiple experimental conditions is required for the finite element updating. This study proposes the new finite element updating method for estimating structural parameters with high accuracy by applying the multiobjective optimization method. This study adopted the satisficing trade-off method (STOM) [8] as the multiobjective optimization method. STOM can obtain a single, highly accurate Pareto solution, regardless of the shape of the Pareto set. Therefore, the method is widely applied to engineering design problems. [9] In addition, part of the authors developed robust and reliability-based multiobjective optimization methods considering uncertainty using STOM. [10), 11)]

Efficiency of the proposed method is verified through the experimental results.

2. Experimental model

The simplified reflector shown in Fig. 3 consists of the simple rib applied the tensional load from a tie cable and a pair of hoop cables. The rib is made of aluminum alloy and the dimension is 1040 mm length with a uniform rectangular cross-sectional shape of 40 mm width and 3 mm thickness. Young's modulus of the rib is obtained from a simple bending experiment as 69.87 GPa. The value is used in the analysis as a constant, not an estimating parameter.

The cables are made of phosphor bronze with 0.3 mm diameter. Tie and hoop cables are connected to the rib at 300 mm and 1000 mm lengths from the hinge center, respectively, through the rod ends. The other ends are fixed at the load cells on the stage to control the tension. The hoop cables are connected with 15 degree inclined from the vertical directions from the rib on the horizontal plane.

Table 1. Load cases

Case	1	2	3	4
Tie cable tension [N]	6.814	7.622	8.418	9.223
Hoop cable tension [N]	34.97	29.94	24.99	19.97

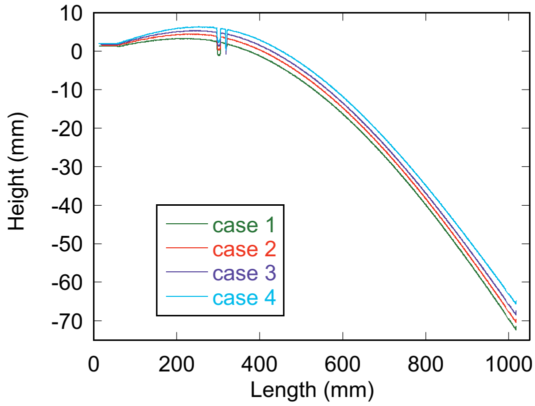

Fig. 4. Deformation obtained by experiment

The rib connected to the hinge is deformed by applying the tension to the connected cables. For the stable deformation to the rib, the cable tension is applied according to the following three steps.

step 1 Only tie cable is connected to the rib. That is, the rib is supported by the hinge and the tie cable and is deformed by the empty weight.

step 2 Then, the hoop cables are connected to the rib. A negligible small tension is applied at the the hoop cables to prevent from the slack.

step 3 The rib is deformed by applying the prescribed tensions to all cables. In order to estimate the parameters, four load conditions are investigated.

In each step, the cable tensions are measured by the load cell and the rib deformation is measured by the laser displacement sensor located on a linear slider with a 0.8 m stroke.

After the steps, the four different cable tensions listed in Table 1 are given to make the rib deformed as different load cases. The deformation distributions in the four cases are shown in Fig. 4. Load case 1 has the largest tip displacement due to the largest hoop cable tensions. On the other hand, the tie cable tension is the smallest of the four cases. This is because the hoop cable tension makes the rib pulled to the hinge direction in addition to the lower direction. Hence, at the tie cable position, the rib is slightly deformed to the upper direction that makes the tie cable tension smaller. The four cases are used to estimate the parameters in the finite element updating. Since uneven deformation near 300 mm is due to the propulsion of the tie cable connecting bolt, the part is not used in the finite element updating.

3. FEM model of rib structure

FEM model of the rib structure is shown in Fig. 5. The rib is modeled by using beam elements and the cables are by cable elements that do not support the compression load as differed from the rod element. The rod ends that is used to connect

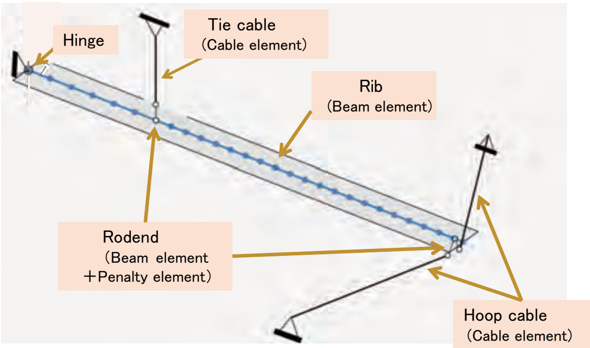

Fig. 5. Finite element model of the one-dimensional simplified rib model

the cables to the rod are modeled by the beam elements. In addition, the penalty element that has rigid in bending with zero length is allocated at each connecting point between the beam and cables for simulating the deformation of the rod end that the connecting angle is always kept perpendicular to the rib on deforming. The rib is equally divided into 28 elements and the structure is modeled by totally 36 elements with 37 nodes.

As boundary conditions, the opposite side edge to the rod end side on the cables is fixed. Cable tensions are obtained as the reaction force and are compared with the experimental results. The hinge of the rib that is opposite side of the hoop cable connecting side is simply supported. However, it is found from the experimental results that the hinge has a small rotational frictions. In order to estimate the unknown friction, the friction is simulated by applying the equivalent moment at the hinge.

The FEM analysis is performed along to the experimental conditions with the three steps loading described in the previous section.

4. Finite Element Updating Using Multiobjective Optimization

Finite element updating is a method to estimate several parameters accurately by changing values of parameters to reduce the difference of structural responses between the finite element analysis and the experimental results. Usually, the optimization method is adopted to minimize the difference, where the RMS error is defined as the objective function in terms of the estimating parameters. Additionally, this study considers multiple experimental conditions for estimating parameters. For the purpose, the multiobjective optimization method is adopted.

The procedure of finite element updating using the multiobjective optimization is shown in Fig. 6 and summarized as follows.

1. At first, the updating parameters is denoted as $\boldsymbol{x} = [x_1 x_2 \cdots x_n]^T$. Set $i = 0$ and the initial estimate value $\boldsymbol{x}_i$
2. The rib deformation $\boldsymbol{u}_f^{(k)}(\boldsymbol{x}_i)$ is evaluated by the geometrically nonlinear finite element analysis, where, k corresponds to the experimental condition.
3. The residual $\boldsymbol{e}_i^{(k)}$ is evaluated as the difference between the deformation shape $\boldsymbol{u}_f^{(k)}(\boldsymbol{x}_i)$ obtained by the analysis and the experimental results, $\boldsymbol{u}_m$.

$$\boldsymbol{e}_i^{(k)}(\boldsymbol{x}_i) = \boldsymbol{u}_f(\boldsymbol{x}_i) - \boldsymbol{u}_m \tag{1}$$

4. Set the objective functions corresponding to the experimental conditions as follows.

$$f_k(\boldsymbol{x}_i) = \sqrt{\frac{1}{2}\boldsymbol{e}_i^{(k)}(\boldsymbol{x}_i)^T\boldsymbol{e}_i^{(k)}(\boldsymbol{x}_i)} \tag{2}$$

f_k corresponds to the RMS error of the rib deformation under the experimental conditions, k, The parameters $\boldsymbol{x}_i$ are updated in the multiobjective optimization step.
5. If the optimization step is converged, the updated parameter is obtained. Otherwise set $i = i + 1$ and go back to step 2.

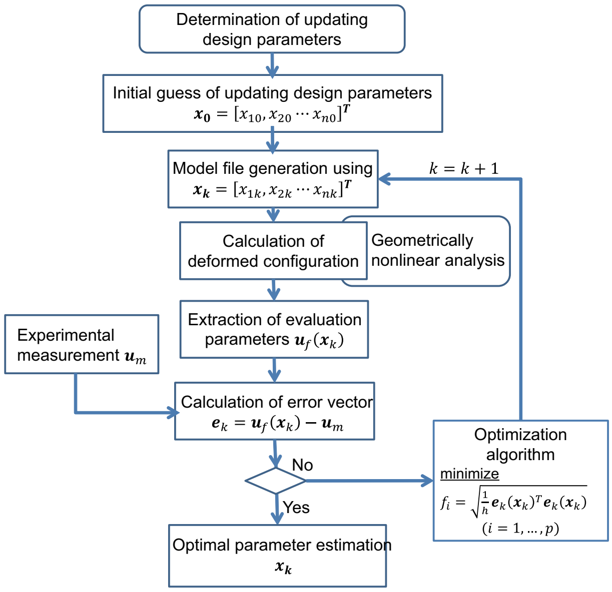

Fig. 6. Flow of finite element model updating using STOM

4.1. Multiobjective Optimization Method

A multiobjective optimization problem is an optimization problem with multiple objective functions.

$$\boldsymbol{f}(\boldsymbol{x}) = [f_1(\boldsymbol{x}), f_2(\boldsymbol{x}), \cdots, f_k(\boldsymbol{x})]^T \tag{3}$$

where k is the number of objective functions, $\boldsymbol{x} = (x_1, x_2, \cdots, x_n)^T$ are the design variables, and n is the number of design variables.

The multiobjective optimization problem is generally formulated as follows:

$$\begin{aligned} \text{Minimize:}\quad & \boldsymbol{f}(\boldsymbol{x}) = [f_1(\boldsymbol{x}), f_2(\boldsymbol{x}), \cdots, f_k(\boldsymbol{x})]^T \\ \text{subject to:}\quad & g_j(\boldsymbol{x}) \le 0 \quad (j = 1, \cdots, m) \\ & x_i^L \le x_i \le x_i^U \quad (i = 1, \cdots, n_x) \end{aligned} \tag{4}$$

where $g_j(\boldsymbol{x})$ $(j = 1, \cdots, m)$ are constraint conditions and x_i^U and x_i^L are the upper and lower limits of the design variables, respectively.

This study adopts the satisficing trade-off method (STOM) as the multiobjective optimization method.[8] STOM is known to be an interactive optimization method that converts a multiobjective optimization problem into the equivalent single-objective optimization problem by introducing an aspiration level that corresponds to the user's preference for each objective function value.

The flow of the STOM is summarized in Fig. 7 and briefly described as follows.

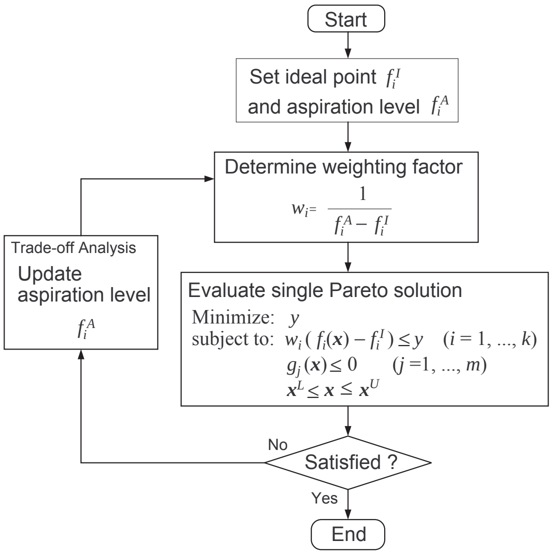

Fig. 7. Flowchart of STOM.

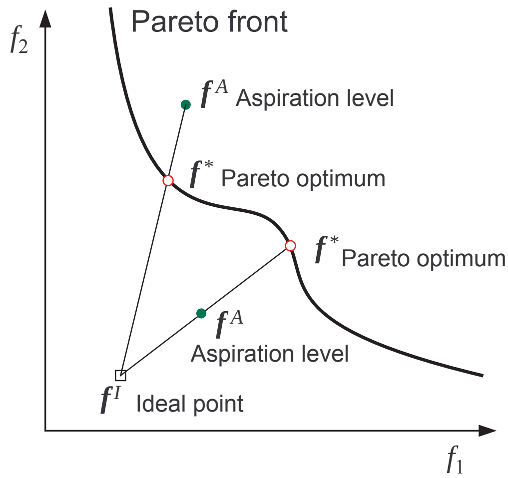

Fig. 8. Pareto solution search process of STOM.

Table 2. Initial and estimated parameter values and RMS error

(a) Initial parameter value and RMS error

Case	1	2	3	4
Moment (Nm)	0	0	0	0
Tie cable tension (N)	6.814	8.566	9.368	9.917
Hoop cable tension (N)	46.12	33.71	28.37	26.75
RMS error (mmRMS)	0.200	0.1851	0.1995	0.1900

(b) Updated parameter value and optimum RMS error

Case	1	2	3	4
Moment (Nm)	0.304	0.0209	0.0149	4.57×10^{-3}
Tie cable tension (N)	5.688	8.120	9.134	10.08
Hoop cable tension (N)	46.11	37.28	30.57	24.63
RMS error (mmRMS)	0.07287	0.07287	0.07286	0.06852

Step 1 Set the ideal point f_i^I, $(i = 1, \cdots, k)$ of each objective function. The ideal point is usually determined by solving a single-objective optimization problem considering only the corresponding objective function, $f_i(\boldsymbol{x})$.

Step 2 Set the aspiration level f_i^A, $(i = 1, \cdots, k)$ of each objective function and evaluate the weight coefficient, w_i, as follows:

$$w_i = \frac{1}{f_i^A - f_i^I} \quad (i = 1, \cdots, k) \tag{5}$$

Step 3 Formulate the multiobjective optimization problem in Eq. (4) into the weighted Tchebyshev norm problem as follows:

$$\begin{aligned} \text{Minimize:} \quad & \max_{i=1,\cdots,k} w_i \left(f_i(\boldsymbol{x}) - f_i^I \right) && (6) \\ \text{subject to:} \quad & g_j(\boldsymbol{x}) \leq 0 \quad (j = 1, \cdots, m) \\ & x_i^L \leq x_i \leq x_i^U \quad (i = 1, \cdots, n_x) \end{aligned}$$

Step 4 The min-max problem in Eq. (6) is transformed into the equivalent single-objective problem by introducing a slack design variable y as follows:

$$\begin{aligned} \text{Minimize:} \quad & y && (7) \\ \text{subject to:} \quad & w_i \left(f_i(\boldsymbol{x}) - f_i^I \right) \leq y \quad (i = 1, 2, \cdots, k) \\ & g_j(\boldsymbol{x}) \leq 0 \quad (j = 1, \cdots, m) \\ & x_i^L \leq x_i \leq x_i^U \quad (i = 1, \cdots, n) \end{aligned}$$

When Eq. (7) is solved using a nonlinear programming method such as a sequential programming method, an accurate Pareto optimal solution is obtained in comparison with an evolutionary method.

Step 5 If the objective function values are satisfactory, the search is completed. Otherwise, update the aspiration level f_i^A and return to Step 2. The automatic trade-off analysis method [12)] is one of the methods used to reasonably update the aspiration level.

The weight coefficient, w_i, plays an important role in obtaining the Pareto solution in the direction of the aspiration level, which is directly related to the designer's preference. As shown in Fig. 8, the Pareto optimal solution is usually located on the line connecting the ideal point and the aspiration level in the objective function space, regardless of whether or not the aspiration level lies in the feasible region. On the other hand, the optimal solution is often not located on the line when some constraints are active. In that case, designers can investigate the effect of the active constraints on the Pareto optimal solution.

5. finite element updating results

On the finite element updating, the four load cases listed in Table 1 are considered and the RMS error of the rib deformation between the experiment and the analysis are defined as objective functions in terms of tie cable and hoop cable tensions as well as the moment at the root hinge that simulates the friction at the hinge. In the STOM, the ideal point f_i^I is set to zero, that corresponds to no error. The aspiration level f_i^A is set to the same value, 0.001 for each case. It corresponds that each case has the same weight.

The initial values of the updating are set as the experimental data for cable tensions and zero of the moment. The RMS errors under the initial conditions are listed in Table 2 (a). The rib deformation distribution under case 1 is compared in Fig. 9. It is found that the FEM results are much different from the experimental results in all cases.

The updated parameter values and the RMS errors are listed

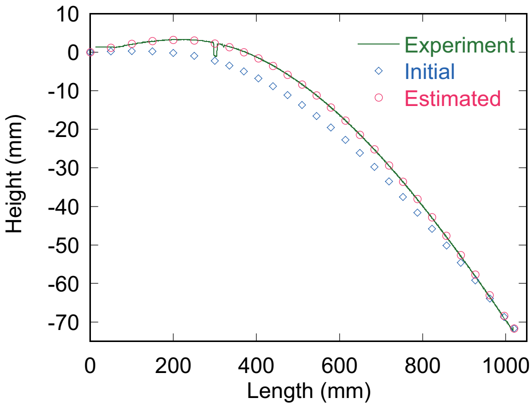

Fig. 9. Comparison of experimental result and FEM analysis using initial and updated parameters in case 1

in Table 2 (b). It is found that the moment at hinge makes the RMS error smaller. Though the hinge ideally has no friction, the friction at the hinge has large effect on the rib deformation on this experiment. On the other hand, the variations of the cable tensions are small. The FEM result using the updated parameters is shown in Fig. 9. It is found that the parameter estimation works well. Due to the limitation of the space, the deformation distribution under other cases are not shown here, but the updating works well for the other cases.

6. Conclusions

This study proposes a finite element updating method using the multiobjective optimization method to consider multiple experimental conditions for estimating parameters. As the multi-objective optimization method, the satisficing trade-off method (STOM) is adopted.

The method is applied to the BBM model for the tension-stabilized space reflector consisting of hoop cables and radial ribs, where the rib is deformed into the prescribed shape by cable tension generated on deployment. It is necessary to estimate the physical parameters in high accuracy to investigate the effect of the parameters on the deformation shape through a geometrically nonlinear finite element analysis.

Through numerical examples, the validity of the proposed method that the analytical deformation shapes are compared with the experimental results is demonstrated. Especially, a friction at the hinge support modeled as the applied moment in the analysis has significant effect on the rib deformation shape.

Acknowledgment

This study is partially supported by JAXA's Strategic Research Grant and JSPS KAKENHI 26249131.

References

1) Higuchi, K., Kishimoto, N., Meguro, A., Tanaka, H., Yoshihara, M. and Iikura, S.: Structure of high precision large deployable reflector for space VLBI (very long baseline interferometry), Proceedings of 50th AIAA/ASME/ASCE/AHS/ASC Structures, Structural Dynamics, and Materials Conference, AIAA-2009-2609 (2009), pp. 1-9.
2) Tanaka, H, Akita, T., Kogiso, N., Ishimura, K., Sakamoto, H., Ogi, Y., and Miyazaki, Y.: A design method for a space antenna structure consisting of radial ribs and hoop cables, Proceedings of 24th JSME Computational Mechanics Conference CMD2011, No. 2326 (2011), pp. 687-688. (in Japanese)
3) Miyazaki, Y., and Tanaka, H.: Elastica solution for simplified model for a space antenna structure consisting of radial ribs and hoop cables, Proceedings of 24th JSME Computational Mechanics Conference CMD2011, No. 2327 (2011), pp. 689-690. (in Japanese)
4) Kogiso, N., Tanaka, H, Akita, T., Ishimura, K., Sakamoto, H., Ogi, Y., Miyazaki, Y., and Iwasa, T.: Comparison of computation accuracy in FEM analysis for a space antenna structural design, Proceedings of 24th JSME Computational Mechanics Conference CMD2011, No. 2328 (2011), pp. 691-693. (in Japanese)
5) Sakamoto, H., Kogiso, N., Tanaka, H., Ishimura, K., and Okuma, M.: Finite-Element Model Updating for Highly Precise Tension-Stabilized Space Reflectors, AIAA 2012-1837, (2012).
6) Friswell, M. I. and Mottershead, J. E.: Finite Element Model Updating in Structural Dynamics, Kluwer Academic Publishers, 1995.
7) Mottershead, J. E., Link, M., and Friswell, M.: The Sensitivity Method in Finite Element Model Updating: A Tutorial, Mechanical Systems and Signal Processing, Vol. 25 (2011), pp. 2275-2296.
8) Nakayama, H., and Sawaragi, Y.: Satisficing trade-off method for multiobjective programming, Lecture Notes in Economics and Mathematical Systems, Vol. 229 (1984), pp. 113-122,
9) Nakayama, H., Kaneshige, K., Takemoto, S., and Watada, Y.: An application of a multi-objective programming technique to construction accuracy control of cable-stayed bridges, European Journal of Operational Research, Vol. 87, No. 3 (1995), pp. 731-738.
10) Toyoda, M. and Kogiso, N.: Robust multiobjective optimization method using satisficing trade-off method, Journal of Mechanical Science and Technology, Vol. 29, No. 4 (2015), pp. 1361-1367.
11) Kogiso, N, Kodama, R. and Toyoda, M.: Reliability-based multiobjective optimization using the satisficing trade-off method, Journals of the Japan Society of Mechanical Engineers, Vol. 1, No. 6 (2014), p. DSM0063.
12) Nakayama, H.: Trade-off analysis using parametric optimization techniques, European Journal of Operational Research, Vol. 60, No. 1 (1992), pp. 87-98.